Sensors and Actuators A 141 (2008) 695–702

Effect of tightening torque on transducer dynamics and bond strength in wire bonding

Lei Han *, Jue Zhong, Gongzhi Gao

Central South University, Changsha 410083, China

Received 11 March 2007; received in revised form 18 July 2007; accepted 3 October 2007
Available online 16 October 2007

Abstract

This study seeks to quantify the screw-fastening effect of the tool/transducer on wire bonding performance. Aluminum wire bonding experiments were performed on a laboratory test bench. Characterizations of bonding process through a wavelet analysis were used to study the relation between screw fastening, vibration behaviors and bond strength. The time–frequency plots were depicted for identifying un-modeled wire bonding dynamics. Finally some statistically time domain features were presented for further analysis.

Keywords: Ultrasonic bonding; Transducer; Laser Doppler vibrometer; Wavelet analysis; Statistics-based data processing

1. Introduction

Wire bonding has been the most widely used and flexible form of interconnecting technology in semiconductor manufacturing [1]. The mechanical reliability of wire bonds in a microelectronic package depends to a big extent on the formation of intermetallic compounds at the interface, environmental stress cycling of the module, fatigue and bonding process itself. Bond process control and bond quality monitoring have been the main concerns for manufacturing OEMs.

Wire bonding is a complex process with many parameters (such as power input, bonding pressure, bonding time, stage temperature, transducer configuration). For such a manufacturing process, to identify main factors and their effects is important for process optimization.

The conventional transducer assembly includes a PZT (lead–zirconate–titanate) driving element coupled at one end, and a bonding tool coupled to the output end of the transducer. For repair/replacement needs, the tool is screw-fastened on the assembly. This is a three-dimensional structure with a "crab-leg"-type bonding tool. Screw-fastening conditions (the torque value on the tool) can affect the transducer performance in packaging practice, but there are few publications dealing with this issue. It was supposed that over-torquing the bonder screw may deform the tip of the transducer while under-torquing may result in inefficient transfer of ultrasonic power, but that needs to be verified.

In our previous study, the wavelet analysis was confirmed to be an effective means to explore bonding process [2]. In this work, we performed aluminum wire bonding to evaluate the effect of the screw fastening in bonding dynamics. Vibration behavior of bonder transducer was monitored, and then wavelet decomposing was utilized to explore the details of bonding process. All wire bonds were shear tested for evaluating the strength formation at different screw-fastening conditions.

2. Transducer/tool dynamics and wavelet analysis

In a conventional transducer assembly (Fig. 1), the output end could be considered as a linear mechanical oscillator and a driver for tool. Our previous experiments confirmed that the PZT transducers are not dynamically very simple [2–6].

Packaging industry has been using the electrical admittance-versus-frequency plot of a PZT/transducer to model its steady-state characteristics. Here conductance is the reciprocal of electrical resistance. Based on if we measure velocity by using laser Doppler vibrometer (LDV) we have the definition for velocity admittance (testing velocity divided by loading voltage). This method is non-contact and more suitable for the 3D structure. Both methods give close resonance peak (Fig. 2),

* Corresponding author. Tel.: +86 731 8877350.
E-mail address: leihanxyz@yahoo.com.cn (L. Han).

0924-4247/$ – see front matter © 2007 Elsevier B.V. All rights reserved.
doi:10.1016/j.sna.2007.10.013

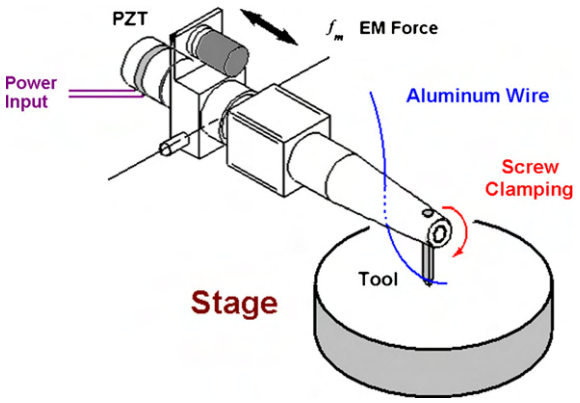

Fig. 1. Wire bonding transducer assembly.

but the resonance peaks were found to shift towards lower frequencies with increasing temperature and/or drive level.

Wire bonding transducer assembly is a special structure with "crab-leg" attachment (bonding tool). It may support many modes of motion except designed longitudinal vibration of transducer. People tend to overlook the bonding tool in transducer dynamics, but the tool plays a critical role that affect energy transfer regardless of its smaller mass and larger stiffness.

The measurements show that inserting of a bonding tool will make the main resonance frequency of transducer assembly lower, and drop the electrical admittance down to approximately half of it [5]. Obtained velocity admittance circle diagram was changed when we change the extended length of the tool (Fig. 3). Obviously the dynamic unbalance by tool is the main reason, which results in up/down bending vibration of the transducer assembly.

Since the ultrasonic loading is provided through tool vibration, when the transducer is operating in non-stationary modes, the above-mentioned behaviors must have act on the bonding target. Next we need to know how they work in a bonding process.

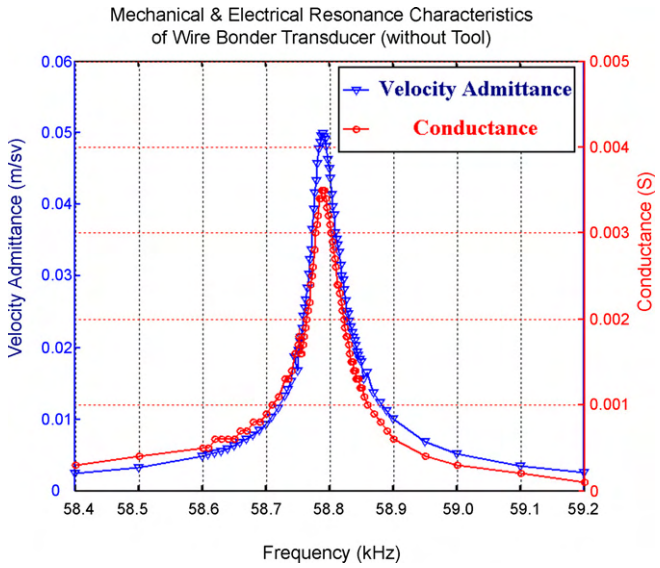

Fig. 2. Velocity and electrical admittance characteristics of transducer (without tool).

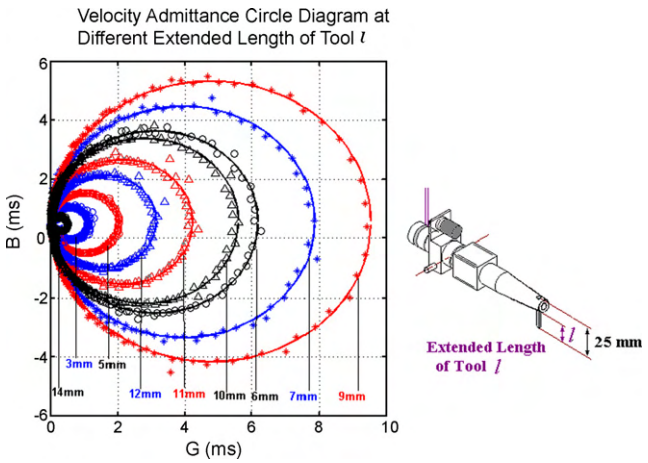

Fig. 3. Velocity admittance characteristics of transducer for different extended length of tool.

Describing a non-linear process, wavelet analysis is proven to be a promising tool due to its capability of time–frequency localization. Time–frequency representations are capable of displaying the time-varying parameters in such a way that relevant information can be extracted [2,7]. For a time-varying signal $f(t)$, the wavelet coefficient of $f(t)$ at scale a and time b is defined by:

$$C(a,b) = \int_R f(t)\frac{1}{\sqrt{a}}\psi\left(\frac{t-b}{a}\right)\mathrm{d}t \quad (1)$$

The selection of a suitable level will depend on the signal and experience. In our case, desired information in wire bonding dynamics may be rapid and small. This signal presents a very quick local variation so the high-frequency and high-sensitive recording will be helpful.

However, there are some limitations to prevent this method to be used directly in our case. Ultrasonic bonding is not strictly an accurate process. These bonding uncertainties may be due to the transducer uncertainties. A single sampled waveform may not exactly represent the typical bonding process. Only the statistics-based feature extraction can circumvent these problems. The uncertainty, if any, can be reduced by repeated measurements while systematic dependent components cannot.

3. Experimental approach

The wire bonding experiments were performed on a U3000 wedge bonder (Weixun Co., Shenzhen) with the working frequency of 57–59 kHz.

Dimension of the transducer (Fig. 4) is: $D_1 = 12$ mm, $D_2 = 8.1$ mm, $D_3 = 19$ mm; $l_1 = 131$ mm, $l_2 = 82$ mm, $l_3 = 65$ mm, $l_4 = 43$ mm, $l_5 = 3.0$ mm, $l_6 = 1.4$ mm. Extended length of the tool (downwards) was 19.5 mm in all tests. Apply a force on the arm end of the wrench for tightening the screw (Fig. 5) for fixing a tool at the transducer end. The product of arm length and tightening force could be used to give a rough magnitude for clamping torque.

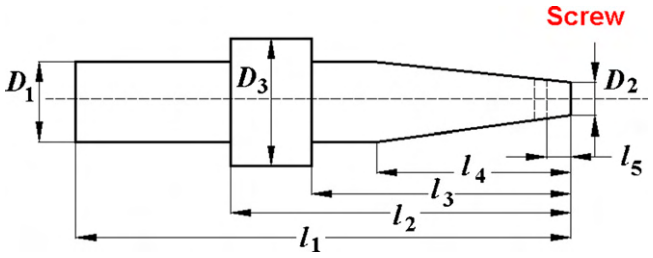

Fig. 4. Dimension of transducer.

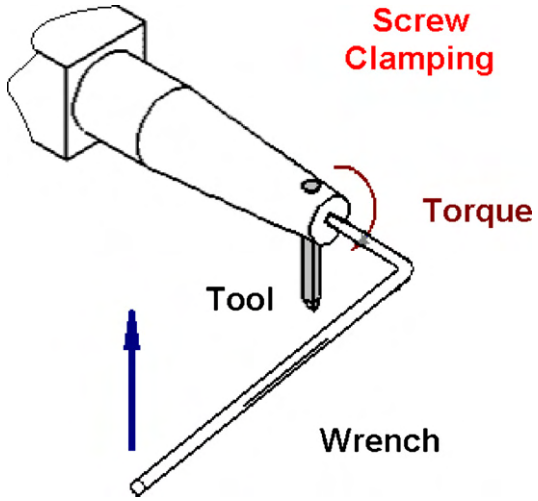

Fig. 5. Wrench for tightening the screw.

The silicon aluminum wire (diameter 300 μm) was bonded onto a nickel-coated aluminum substrate at room temperature. Bonding pressure of 17.4 N was selected to explore the details.

An ultrasonic load initiated after the bond wire was brought down onto the 40 mm × 50 mm × 1 mm substrate by the cemented tungsten carbide wedge. Each bonding took approximately 120–130 ms. The driving voltages and currents to PZT transducer system were recorded by a digital scope and processed off-line.

The effective value power (or RMS power, a statistical measure of the magnitude of varying power during whole process) inputs for 100 repeats were obtained at five clamping settings as shown in Fig. 6.

The bonds were subjected to destructive shear testing at room temperature. Figs. 7 and 8 and Table 1 show the measured shear strength by using the shear apparatus as shown in Fig. 9 at different clamping tightness (each group repeats 200 measurements). Five groups of data were to be selected for analysis of under-bonding, optimal bonding and over-bonding (defined barely enough). The average (mean) strength of bonds at the

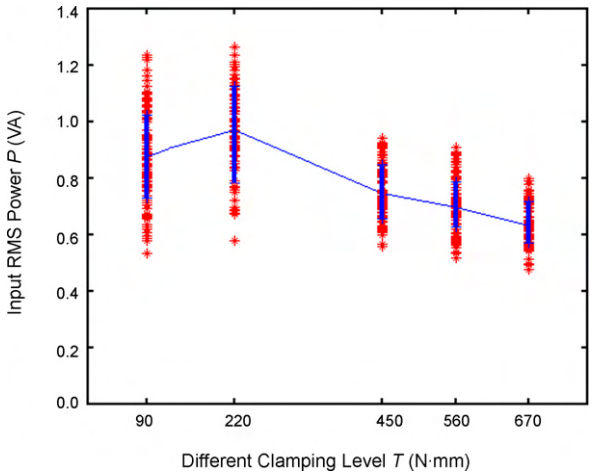

Fig. 6. RMS powers vs. clamping tightness.

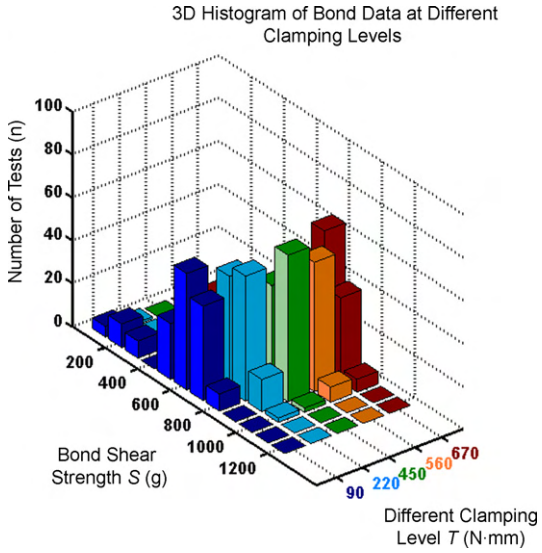

Fig. 7. 3D histogram of bond strength data.

clamping torque of 90 N mm, 220 N mm, 450 N mm, 560 N mm and 670 N mm was 493 g, 655 g, 815 g, 793 g and 735 g, respectively. The optimal bonding happened at the screw torque of 450 N mm but it was not corresponding to the maximal power input (Figs. 6 and 8).

The vibrating transducer/tool was monitored by using a Polytec® PSV-400-M2 laser Doppler vibrometer. The shift in signal beam frequency is related to the vibrating velocity and the wavelength (λ) of the laser through the equation

$$f_s = \frac{2v}{\lambda} \quad (2)$$

Table 1
Statistics of power input and bond strength at different clamping torques

Clamping tightening (N mm)	90	220	450	560	670
Mean of input power W (VA)	0.89	0.97	0.75	0.70	0.63
Standard deviation of input power (VA)	0.16	0.19	0.13	0.12	0.11
Mean strength of bond S (g)	493	655	815	793	735
Standard deviation of strength of bond (g)	167	152	100	99	98

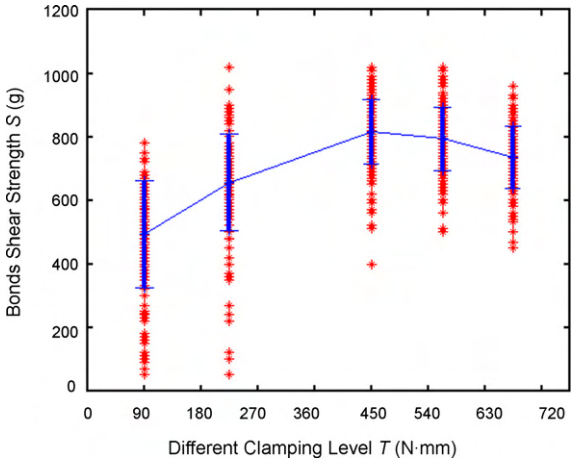

Fig. 8. Bond strength data vs. different clamping torques.

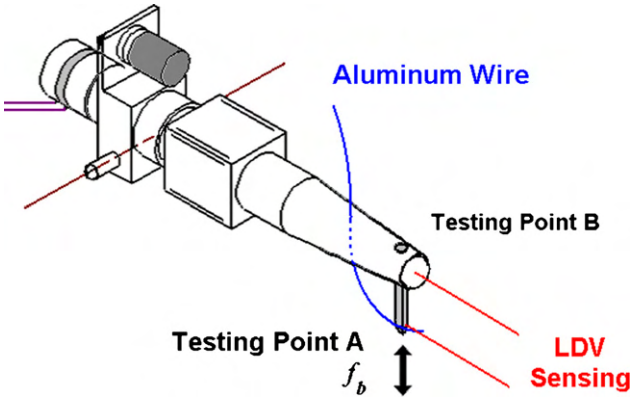

Fig. 10. Testing points for bonding dynamics.

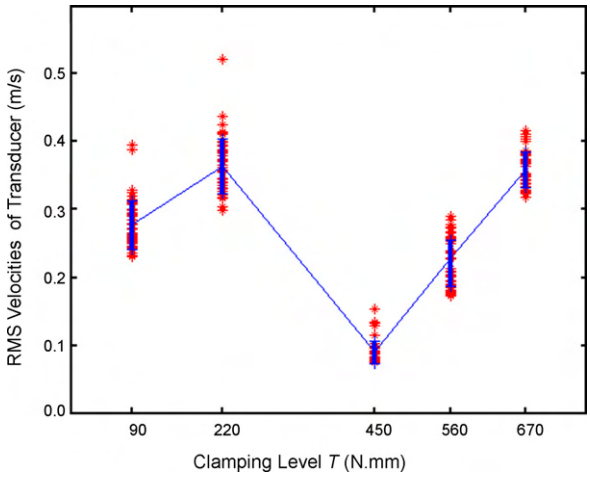

Fig. 11. RMS velocities at B for five clamping torque settings.

where f_s is the frequency shift of the beam and v is the vibrating surface velocity.

Locations A and B (the output ends of tool and transducer) were accessible for LDV sensing and, were conceivable antinodes of linear oscillating, so were selected as the testing points as shown in Fig. 10. The sensing beam of LDV was aligned to the testing point of transducer system. Triggered by the ultrasonic loading signal, the velocity-versus-time profiles then were recorded at a sampling rate of 1 MHz.

Overall (0–125 ms) root mean square (RMS) values of the velocity-versus-time signals gives a measure of effective vibration of transducer/tool under actual bonding conditions.

The averaged RMS transducer velocities (testing point B) and tool velocities (testing point A) at the different screw torque are listed in Table 2 (Figs. 11 and 12). RMS velocity data show that, when screw torque increased, the absolute transducer velocity V_B and the tool velocity V_A changed, whereas the tool velocity (testing point A) was the highest for optimal bonding (Table 2). Experimentally obtained average RMS tool velocities for optimal bonding were approximately 0.336 m/s, corresponding to a displacement of 0.94 μm. For optimal bonding, the experimentally obtained ratio of V_A/V_B was the highest (3.7). Assuming the tool vibrates as the simplest free-free mode, clamping torque modified the tool vibration, as shown in Fig. 13.

It is clear that the bond strength is related to ultrasonic vibrations of the transducer and tool. But one cannot find temporal details by using RMS velocity data.

It is reasonable that a decrease of input power means restricted transducer tool vibration, as described in the last section. However, obtained experimental facts (Tables 1 and 2 and Figs. 7, 8, 11, 12) argued this over-simplified conception. Maximum power input was not corresponding to maximum tangential velocity of tool. Screw-fastening conditions did affect the transducer/tool vibrations.

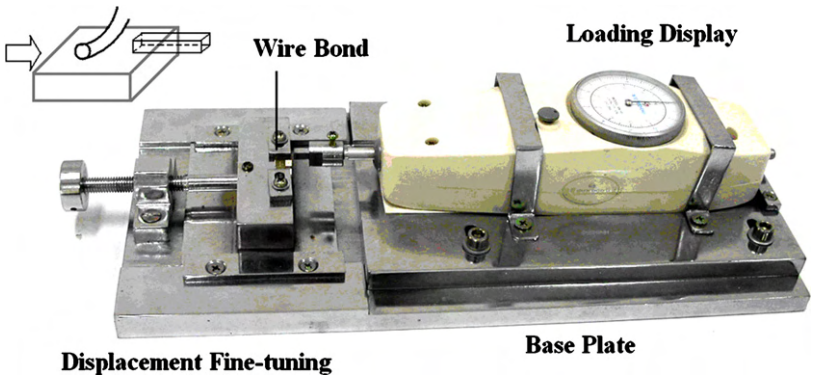

Fig. 9. Bond strength shear testing.

Table 2
Strength of bond, RMS velocities of transducer and tool at different clamping tightness

Clamping tightening (N mm)	90	220	450	560	670
Mean of RMS velocities of tool (m/s)	0.0869	0.103	0.336	0.209	0.0850
Standard deviation of RMS velocities of tool (m/s)	0.029	0.011	0.024	0.036	0.018
Mean of RMS velocities of transducer (m/s)	0.277	0.323	0.090	0.229	0.358
Standard deviation of RMS velocities of transducer (m/s)	0.035	0.041	0.016	0.035	0.026
Ratio of V_A/V_B	0.31	0.32	3.7	0.91	0.24
$V_A + V_B$ (m/s)	0.122	0.144	0.352	0.244	0.111

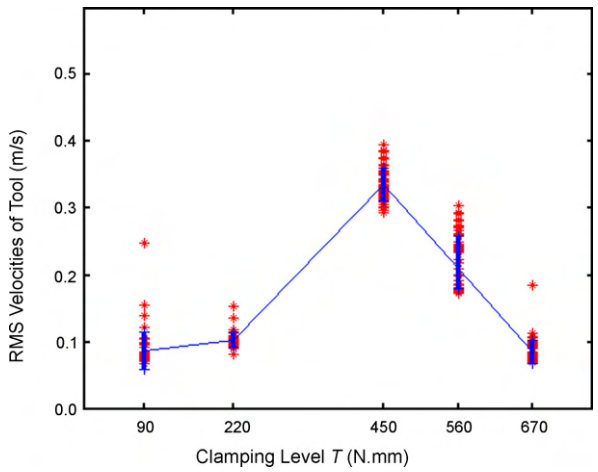

Fig. 12. RMS velocities at A for five clamping torque settings.

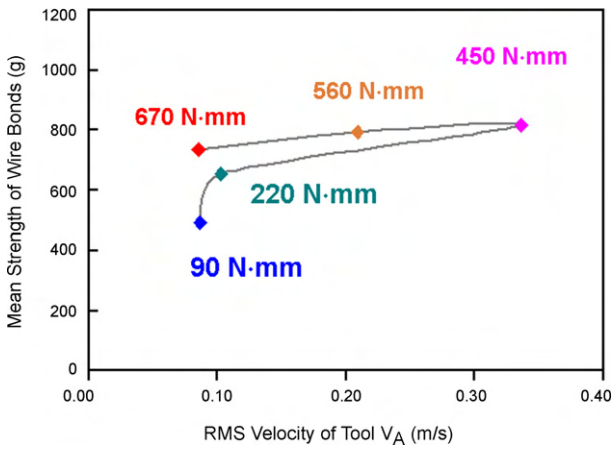

Fig. 14. Bond strength vs. RMS velocities at tool end (testing point A).

Mapping of the correspondences still could be available from the experimentally obtained data. RMS velocity-versus-time as the inputs, and the bond strength the outputs of a bonding process, Fig. 14 gives the relations between the bond strengths and RMS velocities of tool.

It is necessary for us to try to find more temporal details by using other methods.

4. Wavelet decomposition details

The discrete signals were transferred to Matlab for off-line processing. Daubechies invented what are called compactly supported orthonormal wavelets — thus making discrete wavelet analysis practicable. The db30 wavelet was used for its detecting capability of early bonding dynamics [2]. The velocity signal is broken down into five lower resolution components as shown in Fig. 15.

Five components could be available from the original velocity signal as follows:

- D1 — 256–512 kHz
- D2 — 128–256 kHz

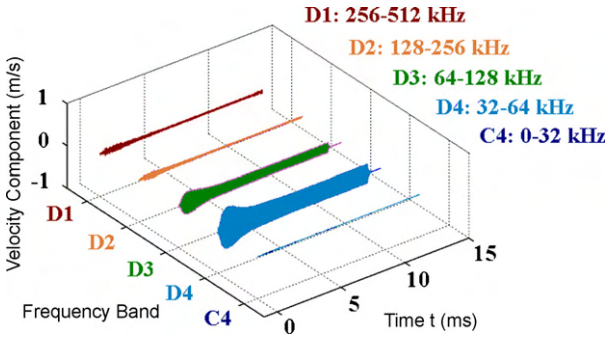

Fig. 15. Wavelet decomposition for a typical original velocity signal.

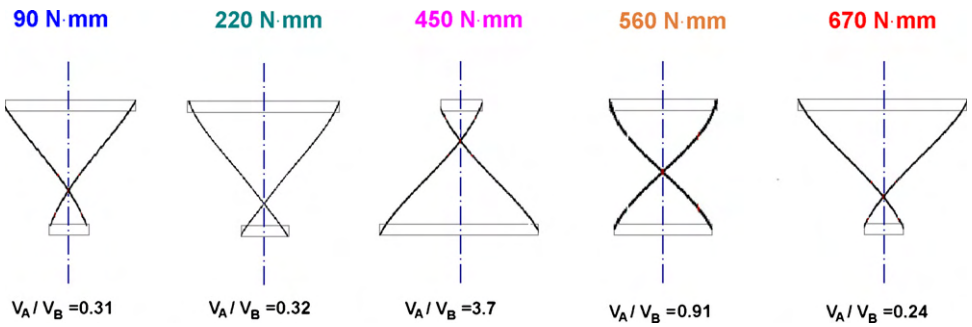

Fig. 13. Presumptive vibration mode of tool based on RMS velocity measurements.

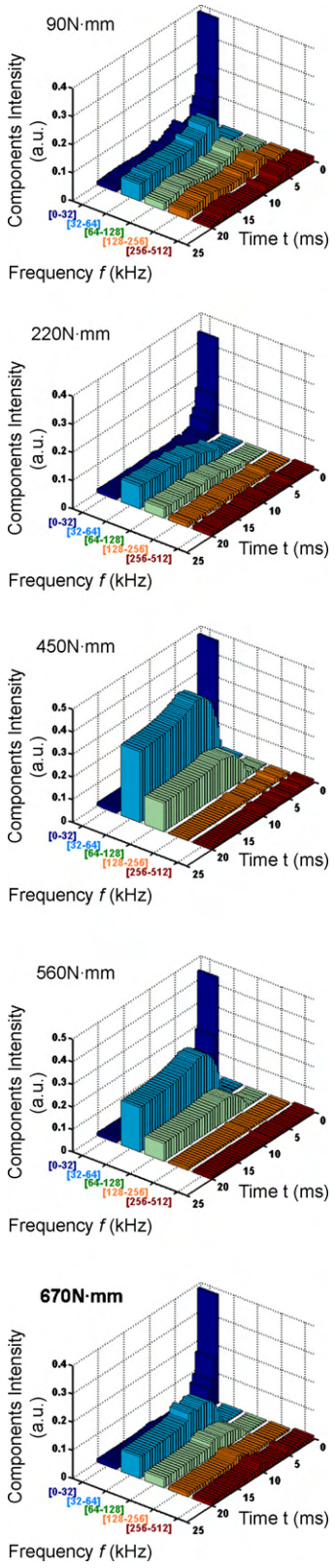

Fig. 16. Three-dimensional time–frequency plot of the wavelet decomposition of tool velocities for different clamping tightening.

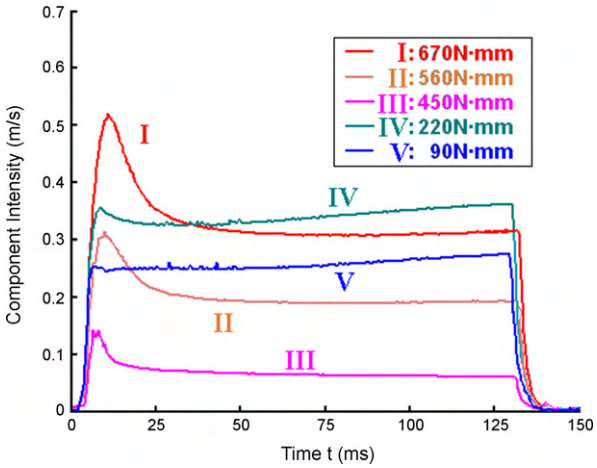

Fig. 17. D4 component-vs.-time plot of transducer velocities for different clamping tightening.

- D3 — 64–128 kHz
- D4 — 32–64 kHz
- C4 — 0–32 kHz

Recording time with a high-quality velocity measurement was 130 ms. For all process (200 repeats at the same bonding condition), 50% of LDV measurements were done for tool vibration (testing point A), 50% for transducer (testing point B). The frequency component was transferred its RMS value (over a period of 50–500 μs), then averaged all RMS value-versus-time profiles over 100 runs for each testing point. More repetition at same condition seemed helpful but not strongly recommended due to the resolution limit of recording device.

Look at the results for testing point A. Fig. 16 contains the 3D "time–frequency" plot of the RMS mean of the wavelet decomposition during 0–20 ms. The picture is looked upon diagonally with time and frequency along the bottom axes in three-dimensional Cartesian space. The vertical axis represents component amplitude.

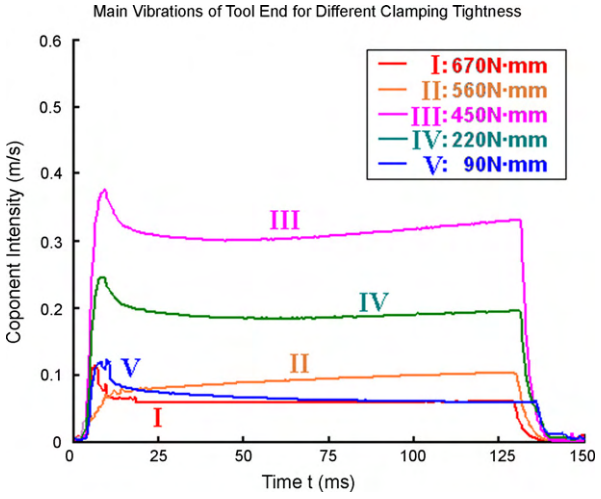

Fig. 18. D4 component-vs.-time plot of tool velocities for different clamping tightening.

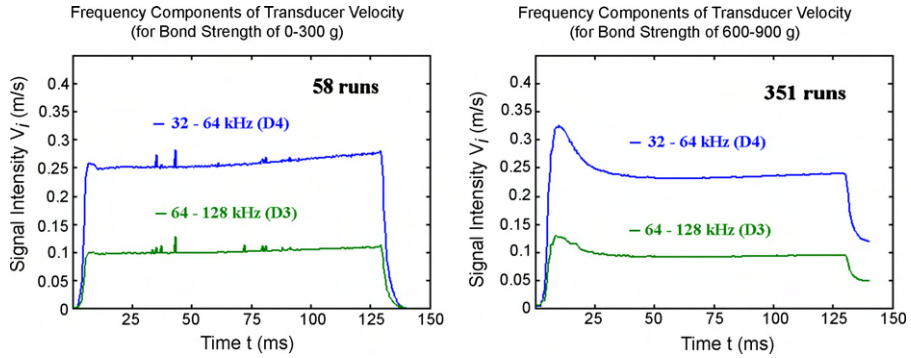

Fig. 19. Average statistical time–frequency plot for poor (left) and good (right) bonding.

C4 component, which includes low frequencies of 0–32 kHz, contained the very high rises during the initial 0–3 ms. The tool with a wire and substrate did not mesh smoothly with each other at the beginning.

The amplitudes of main vibration (57 kHz) of the transducer were different. The transducer velocity for optimal bonding at the screw torque of 450 N mm was the lowest (around 0.1 m/s, see Fig. 17) during the whole bonding process. The tool velocity for optimal bonding at the screw torque of 450 N mm was the highest (around 0.3–0.4 m/s, see Fig. 18). Different clamping torque made the transducer vibration in different ways, especially during the initial 0–20 ms.

The D4 component of tool vibration for 90 and 220 N mm had a smooth plateau (IV and V in Fig. 17), whereas the main component of tool for 450, 560 and 670 N mm (I, II and III) changed at another way. The main velocity curves for higher bond strength reached their peaks at 8–9 ms, then fall gently.

There is another point of view to examine the observed velocity saturation of transducer. From the whole experimentally obtained database, sort out two groups – one group contains all 58 processes with the bonding strength of 0–300 g and another contains 351 processes with the bonding strength of 600–900 g. The time–frequency plots of the wavelet decomposition are shown in Fig. 19. The approximations show this effect clearly: D4 (32–64 kHz frequency band) and D3 (64–128 kHz band) bear a strong resemblance; D4 can be considered as an accurate approximation of the original signal. Main vibrations (32–64 kHz) for good bonding had a same sharp rise then a gentle drop. A period of time 5–25 ms covering the non-stationary vibrations of transducer seemed essential for good bonding.

5. Further results and discussions

Bonder transducer systems may be simplified by breaking up the system into smaller subsystems which are related through the displacement and force conditions at their junction points. Our velocity measurements on bonder transducer provide remarkable difference at various transducer/tool clamping torque. Clamping stress at the junction point (output end of the transducer with a tool) modifies subsystem mode functions as observed in our experiments. Accordingly this structure system does not correspond to a simple combination of longitudinal vibration of transducer and bending vibration of tool.

There was a velocity difference for transducer and tool in Figs. 12 and 13. The vibration mode of tool is likely to change a lot with different screw torque, and a sufficient tool end displacement was needed for optimal bonding in these tests.

The higher frequency vibrations exist particularly at the early stage of a bonding process. The high-frequency vibration of tool at 5–10 ms means something happened in the bonding process. The transducer/tool applies a dynamic tangential load to its target; the opposite reaction modifies the vibration of the transducer assembly. If the lateral force (from the bonding area) was believed as a disturbance for non-linear vibration of tool, a rising of the spectral component may represent an increase of the lateral force. From an intuitive point of view, the duration of 0–30 ms of the process may be relevant to bonding physics. Surface cleaning or peel-off and material softening may be an integrated phase. We were unable to find any direct experimental evidence related to the two distinctly separated segments in Figs. 17–19.

6. Conclusions

The current experimental effort is designed to study the effects of clamping stress in wire bonding. The averaged RMS velocities at a bonder transducer were obtained for evaluating the effects and their influences on bond strength. Screw-fastening conditions did affect the transducer/tool vibrations.

Practical examples of experimentally acquired LDV are used to illustrate the features of the wavelet analysis. For non-stationary wire bonding this procedure offered enhanced capabilities for time–frequency feature extraction and dynamics identification. It minimizes the error in a single shot test, and yields statistical expressions for determining the main factors in a bonding process.

Some important information can be obtained in 3D statistical spectrum analysis based on vibration signals. An unstable contact between aluminum wire and substrate was observed at the initial 0–3 ms. Observed high-frequency tool vibrations may be explained by the lateral resistance provided by the bonding area. An initial increase and following drop of the spectral components may be necessary for good bonding. 3–30 ms of the process may contain important instants for surface cleaning, thorough softening or strength maturation but was insufficient for good bonding in our 300 μm aluminum wire bonding.

Acknowledgements

This work was financially supported by the Natural Science Foundation of China (No. 50575230) and the China Department of Science & Technology Program 973 (No. 2003CB716202). The authors would like to thank Dr. Peter C. K. Liu for helpful discussions.

References

[1] R.R. Tummala, et al., Microelectronics Packaging Handbook [M], Part I, 2nd ed., Chapman & Hall, New York, 1997, pp. I–37–38.
[2] L. Han, R. Gao, J. Zhong, H. Li, Wire bonding dynamics monitoring by wavelet analysis, Sens. Actuators A 137 (2007) 41–50.
[3] L. Han, F. Wang, W. Xu, J. Zhong, Bondability window and power input for wire bonding, Microelectron. Reliability 46 (2006) 610–615.
[4] Y.X. Wu, Z.L. Long, L. Han, J. Zhong, Temperature effect in thermosonic wire bonding, Trans. Nonferrous Metals Soc. China 16 (2006) 622–628.
[5] L. Han, J. Zhong, Nonlinear behaviors of transducer dynamics for thermosonic bonding, in: The 8th IEEE CPMT Conference on High Density Microsystem Design and Packaging and Component Failure Analysis (HDP'06), June 27–30, 2006, Shanghai, 2006, pp. 197–204.
[6] J.-h. Li, L. Han, J.-a. Duan, J. Zhong, Microstructural characteristics of Au/Al bonded interfaces, Mater. Characterization 58 (2007) 103–107.
[7] S. Mallat, A theory for multiresolution signal decomposition: the wavelet representation [J], IEEE Pattern Anal. Machine Intell. 11 (7) (1989) 674–693.

Biographies

Lei Han received the BS, MS and PhD degrees from the University of Science and Technology of China in 1982, 1984 and 1989. He is currently professor of Central South University (China). Research interests are experimental mechanics, smart structures, wavelet analysis and electronics packaging reliability.

Jue Zhong graduated from the Beijing University of Science and Technology (China) in 1958. She is currently professor of Central South University (China) and Fellow of the Chinese Academy of Engineering. Research interests are industrial equipments and microelectronics packaging equipments.

Gongzhi Gao received the BS and MS degrees from Central South University (China) in 2004 and 2007. Research interests are wavelet analysis and electronics packaging reliability.